Multicritical dynamics for the ± J Ising Model

1998 J. Phys. A: Math. Gen. 31 5451

(http://iopscience.iop.org/0305-4470/31/24/007)

J. Phys. A: Math. Gen. **31** (1998) 5451–5465. Printed in the UK PII: S0305-4470(98)92090-X

Multicritical dynamics for the $\pm J$ Ising Model

Yukiyasu Ozeki† and Nobuyasu Ito‡

† Department of Physics, Tokyo Institute of Technology, Oh-okayama, Meguro-ku, Tokyo 152-8551, Japan

‡ Department of Applied Physics, The University of Tokyo, Bunkyo-ku, Hongo, Tokyo 113-8656, Japan

Received 25 February 1998

Abstract. Exact dynamical properties are discussed for the $\pm J$ Ising model around the multicritical point (MCP). It is found that the relation of relaxations between the non-equilibrium remanent magnetization $m(t)$ and the equilibrium autocorrelation function $q(t)$ at the MCP is different from that at the pure critical point. The dynamic critical exponent for the ferromagnetic ordering defined by $m(t) \sim t^{-\lambda_m}$ and that for the spin glass ordering defined by $q(t) \sim t^{-\lambda_q}$ become identical at the MCP. Accurate numerical calculations for them are performed in two and three dimensions using the non-equilibrium relaxation analysis. The MCP is located at $p_{\rm mc} = 0.8872 \pm 0.0008$ and the exponent is estimated as $\lambda_m = \lambda_q = 0.021 \pm 0.001$ for the square lattice. They are estimated as $p_{\rm mc} = 0.7673 \pm 0.0003$ and $\lambda_m = \lambda_q = 0.090 \pm 0.003$ for the simple cubic lattice.

1. Introduction

Recently, the physics of disordered systems has proved a most fascinating subject for theorists and experimentalists. The magnetic materials with impurities such as spin glass (SG) systems are an example of a typical system in this category. In the theory of spin glasses, the mean-field theory presented a unified picture of the SG phase [1, 2]. Studies on the $\pm J$ Ising model in finite dimensions play an important role in the comparison with real spin glasses and the analysis of slow dynamics. It has been used in studies on the existence of the SG transition in $d \geqslant 3$ [3–5], the absence of the re-entrant transition [6–8] and the weak universality of the ferromagnetic (FM) critical exponents [7, 9]. An important issue in real SG materials is the competition between SG and FM orderings, especially the multicritical phenomenon of paramagnetic (PM), FM and SG phases [7, 9–12]. Critical properties for static quantities have been studied explicitly around the multi-critical point (MCP), while those for dynamical quantities remain an open problem at present. Slow dynamics is one of the peculiar properties characterizing the SG phase [13, 14]. The waiting time dependence of relaxation, which is called the ageing, is a typical realization of slow dynamics [15–17]. It has been pointed out that there exists a dynamically singular phase called the Griffiths phase between the critical temperature of the pure FM system and the phase boundary of the low-temperature phase (FM or SG) [18, 19]. Little has been mentioned about the effect of randomness on the dynamic critical phenomena.

The dynamic critical exponent has been investigated for the pure FM system. The dynamic scaling hypothesis reveals a relation between the exponent z and the non-equilibrium critical relaxation of magnetization $m(t)$ [20]. Practically, the relaxation rate is very sensitive to the estimated critical temperature around the true critical point. Thus,

0305-4470/98/245451+15$19.50

one should carefully determine the critical temperature to estimate the exponent precisely. An efficient Monte Carlo technique has been developed to estimate the critical point and the dynamic critical exponent by using the non-equilibrium relaxation of the remanent magnetization from the all-up state [21–25]. It is applied to both two- and three-dimensional systems. For the SG case, the dynamic critical exponent was estimated from the equilibrium autocorrelation function $q(t)$ by Monte Carlo simulations [3, 19, 26]; the power of relaxation for $q(t)$ is related to the exponents associated with the SG ordering. From a similar scaling relation, this power is twice as large as that for $m(t)$ in the pure FM case. The dynamics of these quantities around the MCP has remained an open problem.

In this paper, we study the dynamical properties of the $\pm J$ Ising model around the MCP. Recently, an exact dynamical equation called the ageing relation is developed for Ising spin glasses [27, 28] by using the method of gauge transformation in random spin systems [6, 29, 30]. We derive exact relations for dynamic critical exponents at the MCP using the aging relation. The relation for the powers of relaxation between $m(t)$ and $q(t)$ changes just at the MCP. The relaxation rate of the FM ordering becomes identical with that of the SG ordering. This allows a unified viewpoint of the critical relaxation in the whole parameter region for the $\pm J$ Ising model. We estimate the location of the MCP and the dynamic exponent for two and three dimensions using the non-equilibrium relaxation method.

This paper is organized as follows. In section 2, the model is defined, and the static properties are introduced briefly. In section 3, properties of the critical relaxation are reviewed, and the exact relations for the dynamics around the MCP are derived. Numerical estimations for the MCP and dynamic exponents are presented in section 4. Section 5 is devoted to summary and remarks.

2. Static properties for the $\pm J$ Ising model

The model which we consider is

$$\mathcal{E} = -\sum_{\langle ij \rangle} J_{ij} S_i S_j \qquad (S_i = \pm 1) \tag{2.1}$$

where the summation is taken over all nearest-neighbouring pairs on a lattice; throughout we do not restrict the shape and the dimensions of the lattice, however, one may suppose it as a d-dimensional hypercubic lattice. The exchange interaction J_{ij} is a random variable taking values of $+J$ or $-J$ with the probability distribution

$$P(J_{ij}) = \begin{cases} p & (J_{ij} = J) \\ 1-p & (J_{ij} = -J). \end{cases} \tag{2.2}$$

In three or more dimensions including the mean-field model, the topology of the p–T phase diagram is expected as in figure 1 where the PM, the FM and the SG phases appear [1, 6, 7, 9]. In two dimensions, the SG phase would not exist [1, 3, 4].

The dotted curve indicates the Nishimori-line [6],

$$\frac{J}{k_{\mathrm{B}}T} = \frac{1}{2} \ln \frac{p}{1-p} \tag{2.3}$$

on which the following properties are found.

• The energy and the upper bound of the specific heat are expressed by analytic functions of temperature T.

• The phase boundary between the FM and the SG (or PM) phases below this line would be almost vertical to the p-axis. [7–9, 32]

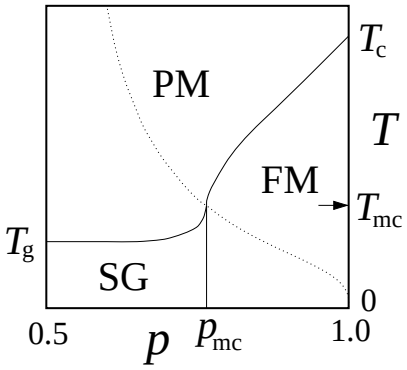

Figure 1. A typical p–T phase diagram for the $\pm J$ Ising model in $d \geqslant 3$. The PM, the FM and SG phases are indicated. The dotted curve is the Nishimori-line.

Table 1. Previous estimations for the location of the MCP in two and three dimensions together with the present results.

Reference	lattice	p_{mc}	T_{mc}	
[7]	square	0.889(2)	0.961(9)	Numerical transfer matrix
[12]	square	0.886(3)	0.975(6)	Series expansion
Present result	square	0.8872(8)	0.970(4)	Non-equilibrium method
[9]	cubic	0.767(2)	1.680(25)	MC Renormalization Group
[10]	cubic	0.7656(20)	1.690(16)	Series expansion
Present result	cubic	0.7673(4)	1.676(3)	Non-equilibrium method

- The line is likely to intersect the MCP.

We define the temperature of the Nishimori-line as T_p from equation (2.3). The shape of phase diagrams are investigated by numerical methods in two [7, 12, 31–33] and three dimensions [9–11]. The locations of the MCP, (p_{mc}, T_{mc}), estimated so far are listed in table 1.

The weak universality, the constantness of $\beta/\nu, \gamma/\nu, \ldots$, for FM critical exponents along the boundary of the FM phase was pointed out by the Monte Carlo renormalization group [9] and numerical transfer matrix calculations [7]. While the series expansion method provided non-universal behaviour for ν just at the MCP [10, 12].

3. Dynamic scaling for the $\pm J$ Ising model

We study the critical relaxation at the MCP using the non-equilibrium process. Dynamic critical exponents have been investigated for the pure FM and the SG cases. First, let us review the critical relaxation for the pure FM case. Some estimations of the dynamic critical exponent z in Monte Carlo simulation have been achieved for the FM critical point owing to the non-equilibrium relaxation of the remanent magnetization [23–25],

$$m(t) \equiv \langle S_i(t) \rangle^{\mathrm{F}} \tag{3.1}$$

where $\langle \cdots \rangle^{\mathrm{F}}$ denotes a dynamical average in which the system is prepared to be the all-up state at $t = 0$, and relaxes in a heat bath of temperature T. The asymptotic behaviour of

$m(t)$ is expected as

$$m(t) \to \begin{cases} m_{\rm eq} & (T < T_{\rm c}) \\ t^{-\lambda_m} & (T = T_{\rm c}) \\ 0 & (T > T_{\rm c}) \end{cases} \tag{3.2}$$

where $m_{\rm eq}$ represents the equilibrium spontaneous magnetization per site. The asymptotic form 0 for $T > T_{\rm c}$ does not mean that the function is always equal to zero but indicates a decay much faster than power-law. Then the dynamic scaling hypothesis [20]

$$m(t, \varepsilon, L) = L^{-\beta/\nu} \bar{m}(L^{1/\nu}\varepsilon, L^{-z}t) \qquad \varepsilon \equiv \frac{T_{\rm c} - T}{T_{\rm c}} \tag{3.3}$$

reveals the relation of exponents

$$\lambda_m = \frac{\beta}{z\nu}. \tag{3.4}$$

Recent accurate estimations for dynamic critical exponents are achieved in this way [23, 24]; for two dimensions, λ_m is estimated to be 0.0577(3), which implies $z = 2.165(10)$ with the exact value, $\beta/\nu = 0.125$ [24] and for three dimensions, $\lambda_m = 0.250(2)$, that is, $z = 2.06(2)$ assuming that $\beta/\nu = 0.515$ [23].

Note that there is another dynamical function, the equilibrium autocorrelation function,

$$q(t) \equiv \langle S_i(t) S_i(0) \rangle_{\rm eq} \tag{3.5}$$

which also decays with a power-law at the FM critical point;

$$q(t) \to \begin{cases} m_{\rm eq}^2 & (T < T_{\rm c}) \\ t^{-\lambda_q} & (T = T_{\rm c}) \\ 0 & (T > T_{\rm c}). \end{cases} \tag{3.6}$$

Using a similar dynamic scaling, one obtains the relation

$$\lambda_q = \frac{2\beta}{z\nu}. \tag{3.7}$$

Thus, λ_m and λ_q are twice as different in the pure FM case.

In the quenched random system, physical quantities are defined as

$$m(t) \equiv [\langle S_i(t) \rangle^{\rm F}]_{\rm c} \tag{3.8}$$

$$q(t) \equiv [\langle S_i(t) S_i(0) \rangle_{\rm eq}]_{\rm c} \tag{3.9}$$

where $[\cdots]_{\rm c}$ denotes the average over quenched bond configurations. The asymptotic behaviour (3.2) and the scaling form (3.3) for $m(t)$ are correct at any critical point along the FM phase boundary. Then we derive the same relation as (3.4) [25]. Note that critical exponents β and ν in these equations are defined with the scaling field $\varepsilon = (T_{\rm c} - T)/T_{\rm c}$. The scaling field is not unique in the random case and one can define another scaling form instead of (3.3) with a different scaling field such as $(p - p_{\rm c})/p_{\rm c}$. However, the ratio β/ν and the exponent z are independent of the scaling field but depend on the critical point itself, as does the relation (3.4). In the FM regime, $p \sim 1$ (see figure 1), we expect that the fluctuation of the spontaneous magnetization among samples of bond configurations does not diverge in the thermodynamic limit even at the critical point except for the MCP. This means

$$[\langle S_i \rangle^2]_{\rm c} = [\langle S_i \rangle]_{\rm c}^2 \tag{3.10}$$

Table 2. Previous estimations for the dynamic critical exponent $\tilde{z}$ for three-dimensional model.

Reference	T_g	λ_q	$\tilde{z}$
[3]	1.2	0.07	5
[19]	1.175	0.065(5)	6.0(8)
[26]	1.175	0.061(9)	5.85(30)

for $N \to \infty$; here we assume that the spontaneous magnetization is measured under infinitesimal magnetic field. If this is true, the asymptotic behaviour (3.6) is also correct in the random case and the same relation as (3.7) holds.

Even on the boundary below the MCP which separates the FM and the SG (or PM) phases, equations (3.2) and (3.3) for $m(t)$ would be correct where the scaling field is modified appropriately. In $d \geqslant 3$, $q(t)$ remains non-zero finite for $t \to \infty$, and gives nothing for the critical relaxation. In $d \geqslant 2$, equations (3.6) and (3.7) would be satisfied if the SG ordering is absent in the vicinity of the FM phase.

In the SG regime, $p \sim \frac{1}{2}$, $m(t)$ does not remain finite for $t \to \infty$ at any temperature, and we have nothing about λ_m. The function $q(t)$ approaches the SG order parameter, q_{SG}. Following the dynamic scaling hypothesis (tilde exponents are those for SG ordering)

$$q(t, \varepsilon, L) = L^{-\tilde{\beta}/\tilde{\nu}} \bar{q}(L^{1/\tilde{\nu}}\varepsilon, L^{-\tilde{z}}t) \tag{3.11}$$

we obtain

$$\lambda_q = \frac{\tilde{\beta}}{\tilde{z}\tilde{\nu}}. \tag{3.12}$$

This exponent was estimated for the three-dimensional system with $p = \frac{1}{2}$ by several Monte Carlo simulations [3, 19, 26] (see table 2).

The relations for FM dynamic exponents, (3.4) and (3.7), would stay along the phase boundaries from the pure case up to the MCP in figure 1, and so does the relation for SG ones (3.12) from $p = \frac{1}{2}$ up to the MCP; it is not clear whether the values of exponents are universal or not. What happens for them just at the MCP? Here we derive exact relations using the ageing relation

$$[\langle S_i(t + t_{\mathrm{w}})S_i(t_{\mathrm{w}})\rangle^{\mathrm{F}}]_{\mathrm{c}} = [\langle S_i(t + t_{\mathrm{w}})S_i(t_{\mathrm{w}})\rangle^{T_p}]_{\mathrm{c}} \tag{3.13}$$

which was previously derived [28] for any concentration p, any temperature T, any waiting time t_{w}, any time interval t and any lattice size. The bracket $\langle\cdots\rangle^{T_p}$ indicates the dynamical average starting from the equilibrium state for the temperature T_p (which is usually different from the temperature of the heat bath T) defined by

$$T_p = \frac{2J/k_{\mathrm{B}}}{\log[p/(1-p)]}. \tag{3.14}$$

On the Nishimori-line ($T = T_p$), $\langle\cdots\rangle^{T_p}$ becomes the equilibrium dynamical average $\langle\cdots\rangle_{\mathrm{eq}}$ [27, 28],

$$\left[\langle S_i(t + t_{\mathrm{w}})S_i(t_{\mathrm{w}})\rangle^{\mathrm{F}}\right]_{\mathrm{c}} = [\langle S_i(t)S_i(0)\rangle_{\mathrm{eq}}]_{\mathrm{c}} = q(t). \tag{3.15}$$

Setting $t_{\mathrm{w}} \to 0$, we obtain an exact dynamical relation along the Nishimori-line,

$$m(t) = q(t). \tag{3.16}$$

With the same scaling forms as (3.3) and (3.11) along $T = T_p$, equation (3.16) provides

$$L^{-\beta/\nu}\bar{m}(L^{1/\nu}\varepsilon, L^{-z}t) = L^{-\tilde{\beta}/\tilde{\nu}}\bar{q}(L^{1/\tilde{\nu}}\varepsilon, L^{-\tilde{z}}t) \tag{3.17}$$

for any L, t and ε (T or p). The scaling field ε in equation (3.17) can be chosen both as $\varepsilon = (p - p_{\rm mc})/p_{\rm mc}$ and as $\varepsilon = (T_{\rm mc} - T)/T_{\rm mc}$ since they are of the same order around the MCP on the Nishimori-line in $d \geqslant 2$. Thus, at the MCP ($\varepsilon = 0$), one obtains

$$\lambda_m = \lambda_q \tag{3.18}$$

$$z = \tilde{z} \tag{3.19}$$

$$\beta/\nu = \tilde{\beta}/\tilde{\nu}. \tag{3.20}$$

Note that the Nishimori-line does not enter the SG phase but just touches it at the MCP [6, 8]. Since exponents $\tilde{\nu}$ and $\tilde{\beta}$ are defined through the scaling field ε and depend on the way to approach the criticality, these exponents in equation (3.17) are not associated with the SG ordering. On the other hand, the dynamic exponent $\tilde{z}$ and the ratio $\tilde{\beta}/\tilde{\nu}$ are defined through the SG correlation length instead of the scaling field. They are independent of the way to approach the criticality, and characterized by the criticality itself. Therefore, exponents $\tilde{z}$ and $\tilde{\beta}/\tilde{\nu}$ are associated with the SG ordering at the MCP. Equations (3.18)–(3.20) relate exponents of FM ordering and SG ordering at the MCP.

The ageing relation is valid for other gauge symmetric systems such as the Sherrington–Kirkpatrick model [34], the gauge glass model and so on [29]. Dynamical relations (3.16)–(3.19) are also valid for these models.

4. Numerical estimations of dynamic critical exponents

In this section, we estimate dynamic critical exponents λ_m at the MCP for two and three dimensions. We perform Monte Carlo simulations for the single spin–flip Metropolis dynamics along the Nishimori-line, and calculate non-equilibrium remanent magnetizations $m(t)$ from the all-up state. We parametrize the points to calculate by the concentration p. The temperature can be obtained by equation (2.3). Because of equation (3.16), this simulation also has the meaning of the calculation for equilibrium autocorrelation functions $q(t)$, and the estimation for λ_q.

Since the relaxation rate is sensitive to the concentration (temperature) around the critical point, we need to estimate it accurately. In the non-equilibrium relaxation, the power-law in the asymptotic regime only appears at the critical point. The local exponent is defined by

$$\lambda(t) \equiv -\frac{{\rm d}\log m(t)}{{\rm d}\log t} \tag{4.1}$$

approaches to λ_m asymptotically at the MCP, while it approaches to 0 or ∞ out of the criticality. Therefore, one can determine the MCP at which the linearity is best in the plot of $\lambda(t)$ to $1/t$. Practically, $\lambda(t)$ is estimated by the least square fitting of $\log m(t)$ to $\log t$ in a finite interval $t - \Delta t < t < t + \Delta t$ of steps, where Δt is chosen appropriately.

In this estimation, it is not necessary to be cautious of the slow relaxation in the Griffiths phase. The Griffiths phase is expected to exist in the region above the low-temperature phases (FM and SG) for $p < 1$. Half of the selected data points in our calculation are located in the Griffiths phase, and the relaxation would be faster than power but slower than exponential on these points. Even so, $\lambda(t)$ approaches ∞ for $t \to \infty$, and the same criterion as in the pure case can be applied.

Since steps for equilibration are not necessary to average physical quantities in non-equilibrium process, these steps can be saved and no difficulties originating from slow relaxation occur even in the simulations for large systems. The finite-size effect is often easily eliminated because the size dependence at fixed time decays exponentially.

Table 3. The parameters of simulations on the square lattice. The number of different bond configurations is denoted by N_b. The simulation is made up to 750 steps for each concentration. For each bond configuration 20 independent runs are performed.

p	lattice size	N_b
0.8830	2501×2500	160
	2001×2000	320
0.8850	2501×2500	320
	2001×2000	320
0.8860	2501×2500	384
0.8865	2501×2500	3648
0.8870	2501×2500	3648
0.8875	2501×2500	3840
0.8880	2501×2500	384
0.8890	2501×2500	160
	2001×2000	320

4.1. Result for two dimensions

Simulations are performed on the square lattice. The typical size is 2501×2500 with the screw boundary condition. Several points of p are selected around the expected MCP on the Nishimori-line to locate the MCP. At each calculation point, we choose several hundred to several thousand independent bond configurations. For each bond configuration, 20 independent Monte Carlo runs are performed. Further, $m(t)$ is averaged over all sites. In total several tens of thousands to hundreds of thousands of samples are used for the statistical average of $m(t)$ for each time step.

The simulation program uses an independent-spin coding technique [35–37] and shuffling technique [38]. Lewis–Payne-type pseudorandom number was used [39, 37, 40]. Details of the program are given in [25]. The simulations are made on Fujitsu VPP500/40, and the performance is 556 MUPS (million update per second) per processor with magnetization counting at every step. The performance becomes 773 MUPS only for spin update.

We observe 750 Monte Carlo steps of $m(t)$ from the all-up state. This time interval is determined in preliminary calculations to resolve the criticality for the present concentration (and the temperature) difference. The details of the simulations are shown in table 3. The number of totally updated spins in the simulation in table 3 is 1.23×10^{15}. It takes about 600 single-processor hours on VPP. Two lattices, 2501×2500 and 2001×2000, are included in table 3. Up to 750 steps, we confirmed that 1501×1500 is large enough for the present accuracy. Thus the results from these lattices are averaged together.

Estimated values of $m(t)$ are shown in figures 2 for three typical values of p. For each point of concentration, $\lambda(t)$ is estimated from the least-square fitting of data in the time interval of 50 steps. Calculated $\lambda(t)$ are plotted in figures 3. It is clearly observed in this figure that the curves for $p \leqslant 0.8865$ turn up when $1/t$ goes to zero—indicating the PM phase in this region—and the curves for $p \geqslant 0.8880$ turn down—indicating the FM phase (see figure 3(*b*)). This means that the critical point exists in $0.8865 < p < 0.8880$. Consequently, the estimated concentration of the MCP is $p_{\mathrm{mc}} = 0.8872 \pm 0.0008$. This means that $T_{\mathrm{mc}} = 0.970 \pm 0.004$. It is consistent with the results of the numerical transfer matrix method $p_{\mathrm{mc}} = 0.889(2)$ and series expansion $p_{\mathrm{mc}} = 0.886(3)$ (see table 1).

Note that the error region ± 0.0008 is not statistical. The extrapolated values of $\lambda(t)$ to $1/t = 0$ can safely be concluded that 0.021 ± 0.001, which is the present estimation for

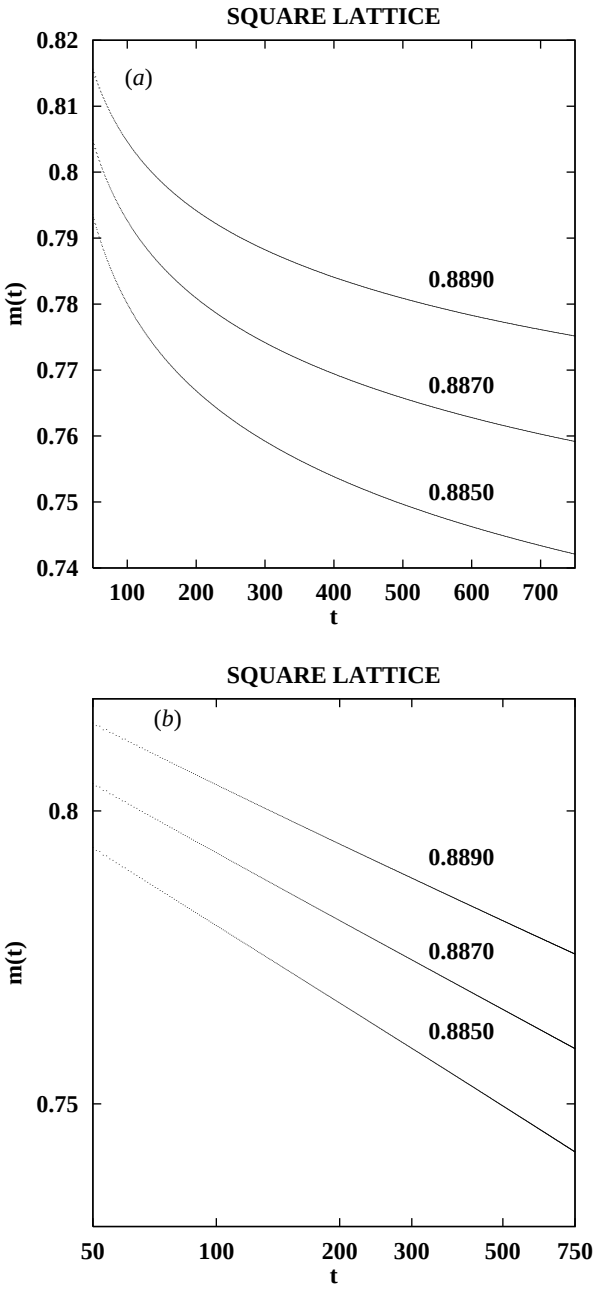

Figure 2. The estimated values of $m(t)$ in two dimensions at three values of p with (a) linear scale and (b) log–log scale. Three curves correspond to $p = 0.885$, 0.887 and 0.889 from bottom to top.

$\lambda_m (= \lambda_q)$. If one assumes the weak universality along the FM phase boundary, $\beta/\nu = \frac{1}{8}$ (the value at $p = 1$) holds and $z = \tilde{z} = 6.0 \pm 0.3$. These exponents are summarized in table 4 together with those obtained so far at other points in the phase diagram. Exponents for the SG ordering make no sense in two dimensions, if no SG phase exists.

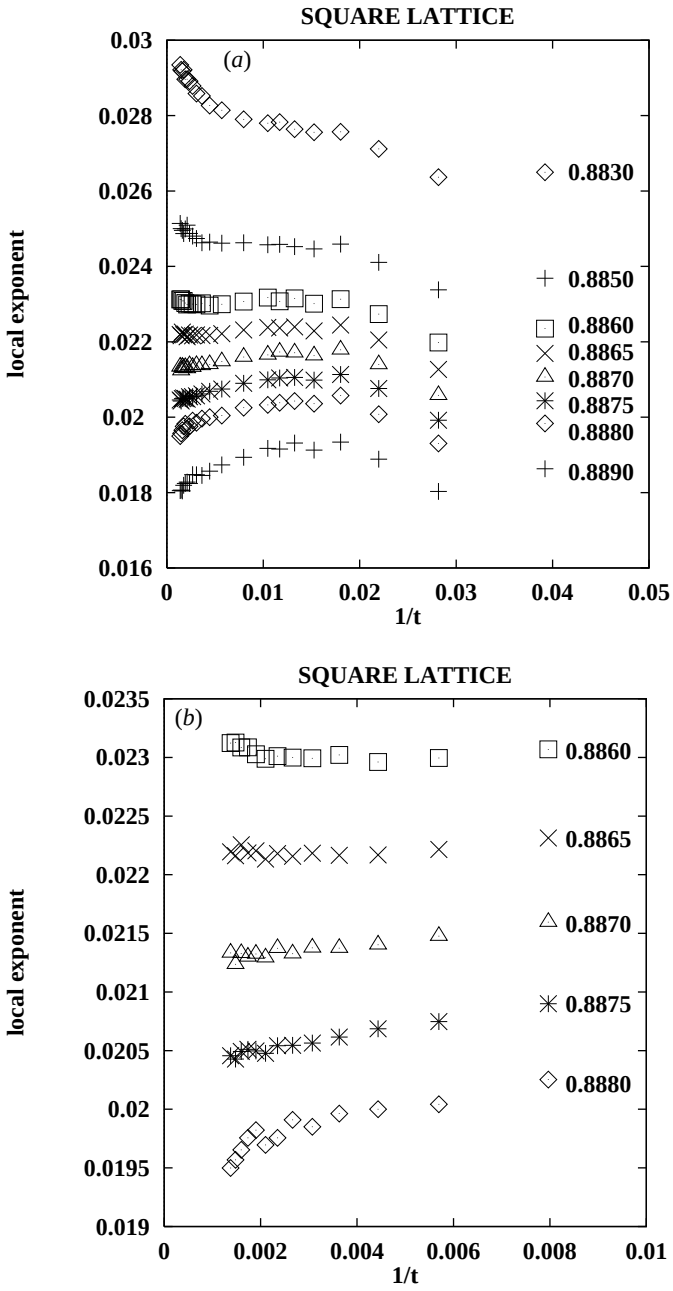

Figure 3. The estimated values of $\lambda(t)$ in two dimensions; (*b*) is a magnified figure of (*a*). The values of p are given in the figures.

4.2. Result for three dimensions

Simulations are performed on the simple cubic lattice. The lattice size is $161 \times 161 \times 162$ with the screw boundary condition. This size is confirmed to be large enough for the

Table 4. The present estimation for the dynamic critical exponent in two dimensions at $p_{\rm mc} = 0.8872$ with the previous estimations at $p = 1$ (the pure FM case) [24].

p	λ_m	λ_q	$z, \tilde{z}$
1	0.0577(3)	0.1154(6)	2.165(10)
$p_{\rm mc}$	0.021(1)	0.021(1)	6.0(3)

Table 5. The parameters of simulations on the simple cubic lattice. The number of bond configurations is denoted by N_b. The simulation is made up to $t_{\rm max}$ steps for each concentration. For each bond configuration, N_r independent runs are performed.

p	$t_{\rm max}$	N_b	N_r
0.7650	2 000	224	5
0.7660	5 000	320	4
0.7665	10 000	800	2
0.7668	10 000	512	10
0.7670	10 000	1312	10
0.7672	20 000	256	5
0.7673	10 000	1024	10
0.7674	20 000	256	5
0.7675	10 000	800	2
0.7677	20 000	256	5
0.7680	5 000	320	4
	10 000	1 600	1
0.7690	5 000	320	4
0.7700	5 000	320	4
0.7710	5 000	320	4
0.7720	5 000	320	4

present precision. The performance on Fujitsu VPP500/40 is 426 MUPS per processor with magnetization counting at every step. It becomes 541 MUPS only for spin update. We execute the simulations listed in table 5. The simulation is made up to $t_{\rm max}$ steps from the all-up state for N_b different bond configurations. For each bond configuration, N_r independent runs are performed. Values of time-dependent magnetization, $m(t)$, is estimated at every step. The number of totally updated spins is 1.89×10^{15}, which takes about 1200 single-processor hours on VPP.

The values of local exponent $\lambda(t)$ are estimated from the least-square fitting of $m(t)$ in the time interval of 50 steps. They are plotted in figures 4. The curves for $p \leqslant 0.7670$ go up when $1/t$ goes to 0 (see figure 4(b)), and those for $p \geqslant 0.7677$ go down (see figure 4(d)). While the data for $p = 0.7670$ in figure 4(b) are somehow subtle to decide the phase, we recognize it in the PM phase because of the upward turns in the closest four points to $1/t = 0$. Therefore the MCP $p_{\rm mc}$ is located in $0.7670 < p_{\rm mc} < 0.7677$. We therefore conclude that $p_{\rm mc} = 0.7673 \pm 0.0003$. This means that $T_{\rm mc} = 1.676 \pm 0.003$. This result is consistent with the results of the Monte Carlo renormalization group method $p_{\rm mc} = 0.767(2)$ and series expansion $p_{\rm mc} = 0.7656(20)$ (see table 1).

The curve of $\lambda(t)$ for $p = 0.7670$ (the lower limit of $p_{\rm mc}$) is extrapolated to 0.093 for $1/t \to 0$, when we neglect the final upward turn (i.e. about seven points close to $1/t = 0$). The curve for $p = 0.7677$ is extrapolated to 0.087 (the upper limit of $p_{\rm mc}$), when we neglect the final downward turn (i.e. about sixteen points close to $1/t = 0$). So we conclude that $\lambda_m = \lambda_q = 0.090 \pm 0.003$. This estimation is easily seen from the extrapolated values of

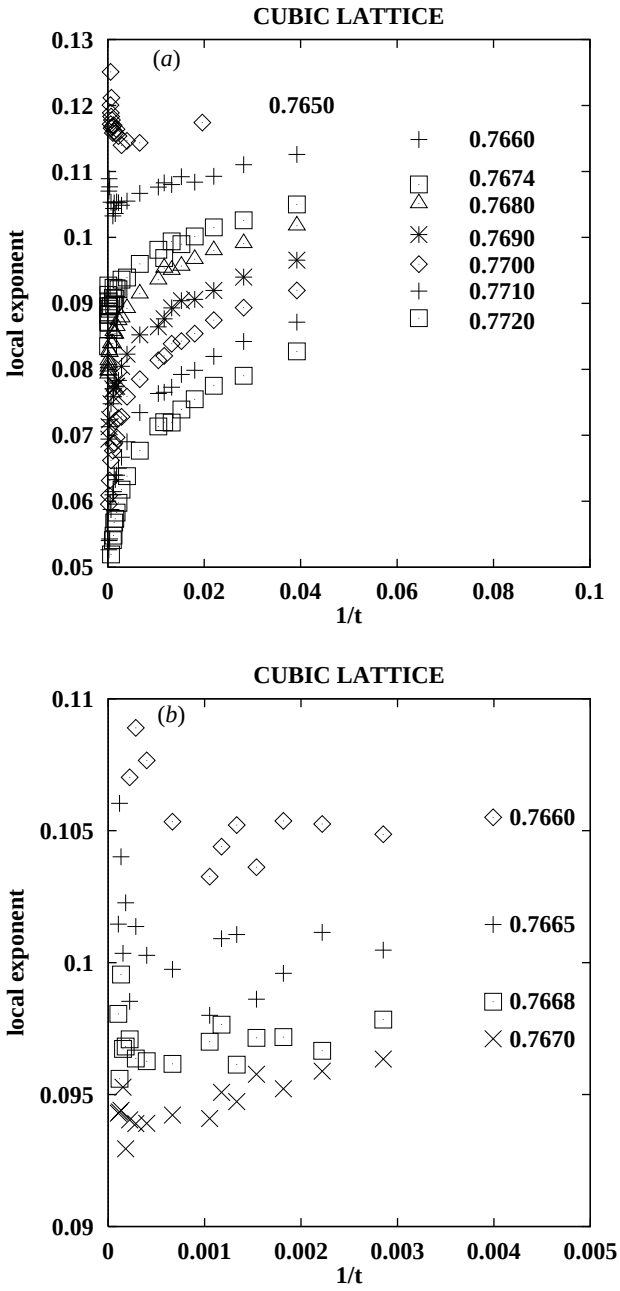

Figure 4. The estimated values of $\lambda(t)$ in three dimensions; (*b*)–(*d*) are magnified figures of (*a*). The values of p are given in the figures.

$\lambda(t)$ in figure 4(*c*) in which all concentrations are close enough to the MCP. If one assumes the weak universality along the FM phase boundary, $\beta/\nu = 0.515$ (the value at $p = 1$) and $z = \tilde{z} = 5.7 \pm 0.2$. These exponents are summarized in table 6 together with those obtained to date at other points in the phase diagram.

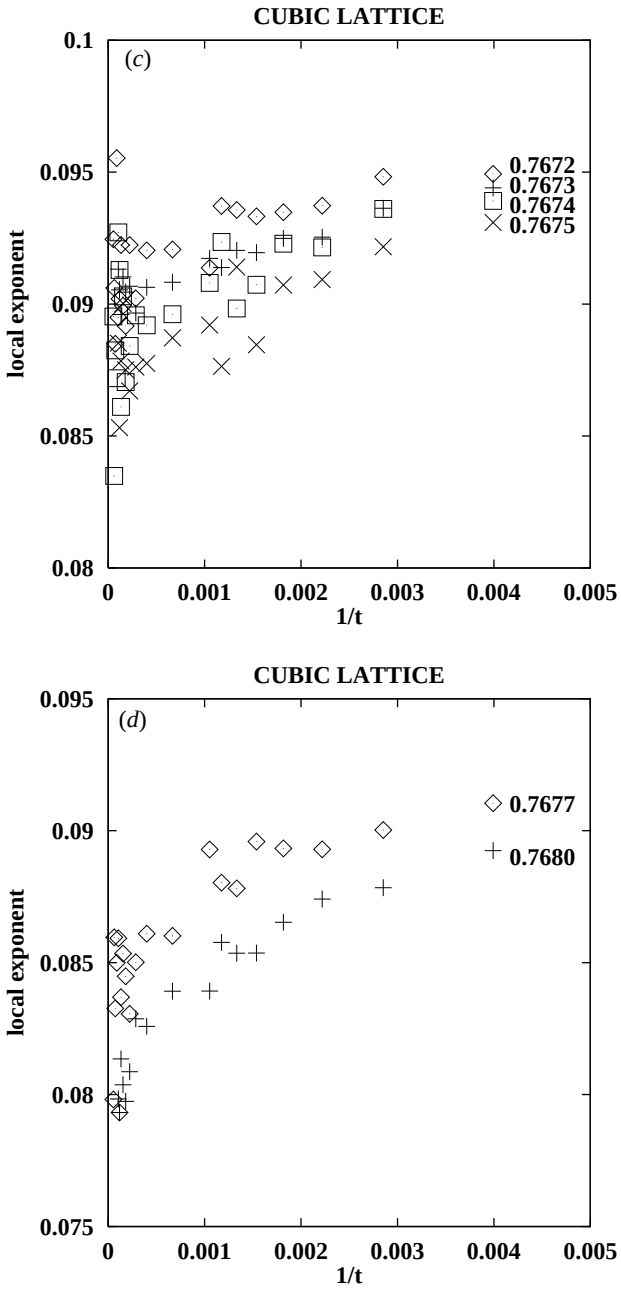

Figure 4. (Continued)

5. Summary and remarks

We examine the dynamical properties around the multicritical point for the $\pm J$ Ising model. The exact equation (3.16) on the Nishimori-line derived from the ageing relation yields the relations (3.18) and (3.19) for dynamic critical exponents of the FM and the SG orderings at

Table 6. The present estimation for the dynamic critical exponent in three dimensions at $p_{mc} = 0.7673$ with the previous estimations at $p = 1$ (the pure FM case) [23] and $p = 0.5$ (the SG case) [26].

p	λ_m	λ_q	$z, \tilde{z}$
1	0.250(2)	0.500(4)	2.06(2)
p_{mc}	0.090(3)	0.090(3)	5.7(2)
0.5		0.061(9)	5.85(30)

the MCP. Analysing the non-equilibrium relaxation of the remanent magnetization calculated by Monte Carlo simulation, we estimate the location of the MCP and the dynamic critical exponent λ_m which is identical with λ_q. Dynamical relations (3.16)–(3.19) are valid for other gauge symmetric systems such as the Sherrington–Kirkpatrick model, the gauge glass model and so on.

The MCP has a peculiar dynamical property,

$$\lambda_q = \lambda_m \tag{5.1}$$

which is different from the pure FM case,

$$\lambda_q = 2\lambda_m. \tag{5.2}$$

As mentioned in section 3, relation (5.2) seems to be correct along the FM phase boundary from $p = 1$ up to the MCP. No such relation exists on the boundary below the temperature of the MCP in $d \geqslant 3$.

It is helpful to consider the asymmetric Mattis model, which can be examined analytically by the gauge transformation technique [41]. The Hamiltonian is similar to equation (2.1);

$$\mathcal{H} = -J \sum_{\langle ij \rangle} \sigma_i \sigma_j S_i S_j. \tag{5.3}$$

The variables $\{\sigma_i\}$ obey the probability distribution

$$P(\{\sigma\}) \propto \exp(-K_0 \sum_{\langle ij \rangle} \sigma_i \sigma_j) \tag{5.4}$$

where $T_0 \equiv J/k_B K_0$ controls the randomness. It is found that the phase diagram has the same topology as in the $\pm J$ Ising model; the multicritical point is located at $(T_0, T) = (T_c, T_c)$. Physical quantities at (T_0, T) are related to those in the pure system. The following relations for $m(t)$ and $q(t)$ at (T_0, T) are easy to derive:

$$m(t) = \langle S_i(t) S_i(0) \rangle^{T_0} \tag{5.5}$$

$$q(t) = \langle S_i(t) S_i(0) \rangle_{eq} \tag{5.6}$$

where averages on the r.h.s. are defined for the pure FM system. Although values of exponents are different between two models, the relation (5.2) is valid along the FM phase boundary up to the MCP, and (5.1) holds at the MCP. Since $q(t)$ remains finite for $t \to \infty$ on the boundary below the MCP, such a relation does not hold. The critical relaxation below the MCP is equivalent to the non-equilibrium relaxation from the equilibrium state at $T = T_c$ to $T < T_c$. We expect this relaxation has the same power-law with critical relaxation.

Dynamic critical exponents are estimated for two and three dimensions by the non-equilibrium relaxation of magnetization calculated by Monte Carlo simulation. This

technique is quite accurate in determining the critical point. The estimated dynamic critical exponent is accurate, while it is very sensitive to the determination of the critical point. From tables 4 and 6, it is indicated that dynamic exponents λ_m and λ_q decrease as the concentration decreases. It would be interesting to know whether these exponents are universal for finite intervals and immediately change at particular concentration(s) or change gradually with the concentration.

The non-equilibrium relaxation method can be applied to other complex phase transitions with slow relaxation. To do so, it is necessary to prepare a (full) ordered state as an initial state of non-equilibrium relaxation. In the case of the SG transition, for example, the equilibrium autocorrelation function $q(t)$ is somehow difficult to calculate accurately, because of the slow relaxation for both equilibration and averaging processes. Furthermore, the preparation of the ordered initial state is not unique nor straightforward. Huse [42] defined an overlap of spin states between the random initial state and the state relaxed in a heat bath,

$$q_0(t) \equiv [\langle S_i(t)S_i(0)\rangle^{\mathrm{R}}]_{\mathrm{c}}. \tag{5.7}$$

However, from the ageing relation (3.13), $q_0(t) = m(t)$ is derived if $p = \frac{1}{2}$. Theoretically, it is not obvious that the critical relaxation for the SG ordering appears in the relaxation of the remanent magnetization. The remanent replica-overlap function,

$$q_{\mathrm{R}}(t) \equiv [\langle S_i^1(t)S_i^2(t)\rangle^{\mathrm{F}}]_{\mathrm{c}} \tag{5.8}$$

could be used as a relaxation function, while the initial state is still out of ordering. Further investigation is necessary in this direction.

Acknowledgments

The simulations have been made using the vector-parallel processor Fujitsu VPP500/40 of ISSP (University of Tokyo). The authors thank Professor A J Bray for helpful discussion.

References

[1] Binder K and Young A P 1986 *Rev. Mod. Phys.* **58** 801
[2] Mezard M, Parisi G and Virasoro A 1987 *Spin Glass Theory and Beyond* (Singapore: World Scientific)
[3] Bhatt R N and Young A P 1985 *Phys. Rev. Lett.* **54** 924
[4] Ogielski A T and Morgenstern I 1985 *Phys. Rev. Lett.* **54** 928
[5] Singh R R P and Chakravarty S 1986 *Phys. Rev. Lett.* **57** 245
[6] Nishimori H 1981 *Prog. Theor. Phys.* **66** 1169
[7] Ozeki Y and Nishimori H 1987 *J. Phys. Soc. Japan* **56** 3265
[8] Kitatani H 1992 *J. Phys. Soc. Japan* **61** 4049
[9] Ozeki Y and Nishimori H 1987 *J. Phys. Soc. Japan* **56** 1568
[10] Singh R R P 1991 *Phys. Rev. Lett.* **67** 899
[11] Ito N 1992 *Computational Approaches in Condensed-matter Physics* ed S Miyashita, M Imada and H Takayama (Berlin: Springer) p 236
[12] Singh R R P and Adler J 1996 *Phys. Rev.* B **54** 364
[13] Fischer K H and Hertz J A 1991 *Spin Glasses* (Cambridge: Cambridge University Press)
[14] Takayama H 1995 *Computational Physics as a New Frontier in Condensed Matter Research* (Physical Society of Japan) p 230
[15] Lundgren L, Svedlindh P, Nordblad P and Beckman O 1983 *Phys. Rev. Lett.* **51** 911
[16] Vincent E, Hammann J and Ocio M 1992 *Recent Progress in Random Magnets* ed D H Ryan (Singapore: World Scientific) p 207
[17] Rieger H 1993 *J. Phys. A: Math. Gen.* **26** L615
[18] Griffiths R B 1969 *Phys. Rev. Lett.* **23** 17

[19] Ogielski A T 1985 *Phys. Rev.* B **32** 7384
[20] Suzuki M 1976 *Phys. Lett.* **58A** 435
[21] Stauffer D 1992 *Physica* **186A** 197
[22] Kohring G A and Stauffer D 1992 *Int. J. Mod. Phys.* C **3** 1165
[23] Ito N 1993 *Physica* **192A** 604
[24] Ito N 1993 *Physica* **196A** 591
[25] Ito N, Matsuhisa T and Kitatani H 1998 *J. Phys. Soc. Japan* **67** 1188
[26] Blundell R E, Humayun K and Bray A J 1992 *J. Phys. A: Math. Gen.* **25** L733
[27] Ozeki Y 1995 *J. Phys. A: Math. Gen.* **28** 3645
[28] Ozeki Y 1997 *J. Phys.: Condens. Matter* **10** 11 171
[29] Ozeki Y and Nishimori H 1993 *J. Phys. A: Math. Gen.* **26** 3399
[30] Ozeki Y 1996 *Statistical Models, Yang-Baxter Equation and Related Topics* ed M L Ge and F Y Wu (Singapore: World Scientific) p 277
[31] Kitatani H and Oguchi T 1990 *J. Phys. Soc. Japan* **59** 3823
[32] Ueno Y and Ozeki Y 1991 *J. Stat. Phys.* **64** 227
[33] Ozeki Y 1993 *J. Phys. Soc. Japan* **62** 2641
[34] Sherrington D and Kirkpatrick S 1975 *Phys. Rev. Lett.* **35** 1972
[35] Michael C 1986 *Phys. Rev.* **33** 7861
[36] Ito N and Kanada Y 1988 *Supercomputer* **5** 31
[37] Ito N and Kanada Y 1990 *Proc. Supercomputing '90 (New York) (Supercomputer **7** 29)* (Los Alamitos, CA: IEEE Computer Society)
[38] Ito N, Kikuchi M and Okabe Y 1993 *Int. J. Mod. Phys.* C **4** 569
[39] Lewis T S and Payne W H 1973 *J. ACM* **20** 456
[40] Ito N and Kanada Y 1990 *Supercomputer* **7** 29
[41] Ozeki Y 1993 *J. Stat. Phys.* **71** 759
[42] Huse D A 1989 *Phys. Rev.* B **40** 304